Endothelial glycocalyx hyaluronan biosynthesis and function in microcirculation

Wang, G.

CHAPTER 5

5

The glycolytic activator PFKFB3 regulates glycocalyx synthesis and thereby vessel stability in tumor endothelium

Gangqi Wang, Bernard M. van den Berg, Anna Rita Cantelmo, Sarantos Kostidis, Wendy M.P.J. Sol, Martin Giera, Peter Carmeliet and Ton J. Rabelink

Abstract

Hyaluronan is one of the main structural constituents of the endothelial glycocalyx. Our previous work showed that the integrity of this layer is critical for vessel wall stability, where hyaluronan in the glycocalyx serves a as conditional matrix for angiopoietin signalling. Here we study the metabolic regulation of hyaluronan (HA) synthesis in tumor endothelial cells. Endothelium in tumor vessels in metastatic melanoma are characterized by increased glycolysis and reduced endothelial surface hyaluronan. We show that increased glycolysis in tumor endothelial cells results in reduced flux into the hexosamine and glucuronic biosynthetic pathways and hence reduced cytosolic concentrations of the HA substrates UDP-GlcA and UDP-GlcNAc, thus hampering endothelial HA synthesis. This reprioritization of HA synthesis substrate into the glycolysis pathway is shown to be dependent upon increased activity of the glycolytic activator PFKFB3. In support, tumor vessels in mice that are haplo-insufficient for PFKFB3 in endothelial cells have normalized endothelial surface hyaluronan and normal angiopoietin signalling and vessel stability. These data show a direct link between glucose fluxes, glycocalyx synthesis and vessel stability in tumor endothelium, and further suggest that restoration of endothelial glycocalyx function by manipulating glycolysis could be a target to achieve vessel normalization.

Introduction

All cells in the body are covered with a glycocalyx layer (GL), a carbohydrate-gel composed of the glycosaminoglycans heparan sulfate (HS), hyaluronan (HA), chondroitin sulfate and associated proteins [1]. The GL is especially critical for the homeostasis of the vasculature. Indeed, the GL controls vessel perfusion, ensures vessel patency (through its anti-thrombotic properties), regulates vascular barrier permeability, impairs cancer cell adhesion and extravasation, and prevents vascular inflammation (through precluding leukocyte adhesion to endothelial cells (ECs)) [2-4]. Damage of the endothelial GL is associated with vascular destabilization in cancer, diabetes and other life-threatening diseases such as sepsis [5-7]. Despite its importance, the GL is one of the most understudied structures in vascular biology and understanding of its regulation and role in vascular homeostasis is still very limited [8]

Recent studies highlighted the importance of EC metabolism in angiogenesis in health and disease, and illustrated that targeting EC metabolic targets inhibits pathological angiogenesis in inflammatory and malignant diseases in preclinical mouse models [9-11]. We recently reported that lowering EC glycolysis induced tumor vessel normalization, thereby reducing metastasis and improving chemotherapy [9]. Whether EC metabolism regulates the production of the GL has never been explored.

In tumors, vessels are structurally and functionally abnormal, characterized by EC destabilization [12], while in diabetes, ECs are dysfunctional with vascular barrier defects and enhanced leukocyte adhesion [13]. Tumor vessel destabilization impairs tumor perfusion, promotes cancer cell intravasation and dissemination, and compromises the delivery and efficacy of chemo-, radio- and immunotherapy [14]. Strategies promoting tumor vessel normalization reduce metastasis, while promoting anti-cancer therapy responses are increased [9, 15]. Whether strategies targeting EC metabolism can promote the formation of the endothelial GL is unknown.

The GL also importantly regulates binding of growth factors and other biologically important molecules to the EC surface [16, 17]. In contrast to heparan sulfates, HA lacks the specific chemical modifications (i.e., sulfation, acetylation, and epimerization), implicated in protein and growth factor binding [18]. Remarkably, glycocalyx research has been mostly centered around the heparan sulfate (HS) component [2]. The ubiquitous distribution of HA *in vivo*, the biological activity of HA fragments when using degradative enzymes [19], and the inability to specifically inhibit HA synthesis *in vivo* have hampered the study of the potential role of HA in endothelial glycocalyx function to date.

HA is a linear polysaccharide that is composed of repeating units of glucuronic acid (GlcA) and N-acetyl-glucosamine (GlcNAc) linked together through glycosidic bonds that can be repeated several thousand times, thus requiring very large amounts of substrates. Starting both from the glycolytic intermediate

glucose-6-phosphate, the glucuronic acid biosynthesis pathway produces GlcA, while the hexosamine biosynthesis pathway produces GlcNAc [20]. In contrast to the synthesis of other glycosaminoglycans, which takes place in the Golgi system, HA is produced at the plasma membrane using the cytoplasmic substrate pool. Therefore, cytosolic uridine diphospho-glucuronic acid (UDP-GlcA) and UDP-GlcNAc availability is critical for this energy consuming process, rendering the metabolic state of the cell an important factor for production of HA [21-25]. This may be even more relevant in ECs where an inherent high rate of glycolysis may shift glucose-6-phosphate away from the metabolic pathways that produce the HA substrates UDP-GlcA and UDP-GlcNAc. [11, 26]. We therefore hypothesize that in tumor endothelium, HA-glycocalyx synthesis is impaired, and that this dysregulated synthesis is related to hyper glycolysis.

A key regulator of endothelial quiescence and maintenance of the endothelial barrier function is angiopoietin 1 (Ang1), a secreted ligand of the endothelial Tie-2 kinase [27, 28]. Adult tissues, such as brain, heart and especially glomerular fenestrated and retinal endothelium constitutively show Ang1 signalling [29, 30]. We recently, described that Ang1 needs to bind to HA in the endothelial ECM to allow for proper signalling [31]. Whether, disturbed HA synthesis related to altered glucose metabolism also results in impaired vessel stabilisation by Ang1 is unknown, but would be of great relevance to understand processes such as tumor metastasis.

In this study, we explored whether manipulation of endothelial glycolysis can regulate GL formation. Our findings may have therapeutic relevance to induce vessel normalization and EC stabilization by promoting GL formation through inhibition of EC glycolysis.

Methods

Reagents

All materials are from Sigma-Aldrich (St. Louis, MO, USA) or stated otherwise.

Mice

C57BL/6 (WT, 7-9 weeks old) and *Pfkfb3*$^{+/\Delta EC}$ mice[9], used for the metastatic mouse model, were from the KU Leuven Animal Facility. Animal procedures were approved by the Institutional Animal Care and Research Advisory Committee (KU Leuven) (permit ECD207/2014) and were performed in accordance with the institutional and national guidelines and regulations. B16-F10 mouse melanoma cells were injected intravenously via the portal vein to obtain liver tumors[9, 32]. After anesthesia (100mg/kg ketamine and 10mg/kg xylazine), median laparotomy was performed, the hilum of the liver was exposed and 150,000 melanoma cells were injected in a volume of 100µL PBS into the portal vein

using a 32 G needle. After the injection, a cotton swab was placed on the lesion until the bleeding stopped. In case of persistent bleeding, a cellulose fleece was placed on the injection site. After injection, the intestine was replaced and the abdominal wall was closed in a two-layer technique. The animals were sacrificed 12 days' post-injection and liver tissue containing metastases were placed in 4% paraformaldehyde solution for further processing. Normal liver tissue was examined as control of the metastases. All animals had free access to standard chow and tap water.

Immunohistochemistry

Deparaffinized liver sections (4 µm thick), were washed in PBS and antigen retrieval was performed in a Tris-EDTA (pH 9.0) buffer in an autoclave. Slides were incubated with 3% H2O2 for 15 minutes at rT and after washing with 0.01% Triton-X100 in PBS, blocked in Serum-Free Protein Block buffer (X0909, Dako) for 1hr at rT. Primary Goat anti-mouse Ang1 (AF923, R&D Systems), CD31 antibody (ab28364, Abcam), HA binding peptide Neurocan-dsRed (200 µg/mL), or lectin from Bandeiraea simplicifolia isolectin B4 (BS-1-TRITC, L5264, Sigma or BS-1-BIOTIN, L2140, Sigma) were incubated overnight at 4°C in blocking buffer, followed by an appropriate secondary antibodies for 1 hour at rT, washed with PBS. Tissue slides were embedded in ProlongTM gold antifade mountant with DAPI (P36931, ThermoFisher) and recorded using a 3D Histech Pannoramic MIDI Scanner (Sysmex). For Tie2 receptor labeling samples were, after blocking with Serum-Free Protein Block buffer, incubated with 3% normal goat serum (NGS), 1% BSA and 0.3% Triton X-100 and incubated with Goat anti-Pospho-Tie2 (Y1102/Y1100; AF3909, R&D Systems) and Mouse anti-Tie2 (ab24859, Abcam), overnight at 4°C followed by Rabbit Anti-Goat-IgG-HRP (Dako) for 30 minutes at rT. Samples were rinsed with PBS containing 0.1% Tween-20, and incubated for 10 minutes with TSA-Cy3 (Perkin Elmer) diluted in TSA dilution buffer (TSA Plus Cyanine 3 System, NEL744001KT, Perkin Elmer). Next, samples were rinsed with PBS-0.1% Tween-20, incubated with secondary Goat anti-Mouse-IgG1-AF488 (Mol Probes) for 1hr at rT and embedded with ProLong® Gold Antifade Reagent containing DAPI (Cell Signaling Technology). Tissue slides were recorded using a 3D Histech Pannoramic MIDI Scanner and a 40x objective lens (Plan Apochromat, NA 0.95). Staining area is quantified using ImageJ software and displayed as percentage p-Tie2 / Tie2 ratio (n = 4 WT or 5 Pfkfb3+/ΔEC).

Creation of Neurocan-dsRed construct

The N-terminus rat neurocan construct of the hyaluronan specific neurocan-eGFP (Ncan-eGFP, gift from J. Kappler) construct [33], linked to the BM 40 signal peptide with APLGRGSHHHHHHGGLA and a GSSGA linker at the C-terminus, was excised and fused into a pDsRedMonoN1 (ClonTech, Mountain View, CA, USA) plasmid. The modified neurocan-dsRed (Ncan-dsRed) construct was incorporated into a self-inactivating (SIN) lentiviral vector (pLV-CMV-IE.Ncan-dsRed) and transduced into Hek293 cells

for production. Ncan-dsRed was isolated from supernatant and purified on a Ni-NTA resin column using the incorporated 6xHistidine tag within the protein.

Tissue slice imaging

In a similar fashion the liver-tissue slices were examined. For each image, the amount and location of intensity profiles were quantified by estimating the distance from CD31 peak signal to the half-width of the intraluminal Ncan-dsRed (liver, n = 4; metastasis, n = 6), or LEA-FITC (liver, n = 3; metastasis, n = 6) fluorescence along the lines of interest (5 per image, line width 5 pixels). Total luminal endothelial fluorescence was calculated from fluorescence within this section. Per slice at least 3 images of blood vessels were analyzed.

Cell isolation and culture

Primary human umbilical vein endothelial cells (HUVECs) were freshly isolated, by perfusion and subsequent incubation (20 minutes) of trypsin at 37°C, from different donors as described[34] (with approval of the Medical Ethical Commission of the Leiden University Medical Center, and informed consent from all subjects) and used between passage 1 and 3. Freshly isolated HUVECs were cultured on 0.5% gelatin–coated plastic flasks in endothelial basal medium (CC-3121; Lonza, Basel, Switzerland), supplemented with human epidermal growth factor, vascular endothelial growth factor, human fibroblast growth factor-B, R3-IGF-I, ascorbic acid, heparin, and 10% human serum (Lonza, Basel, Switzerland) supplemented with antibiotics/antimycotics (Life technology, Gibco).

In vitro culture experiments

After transduction with either lentiviral- or adenoviral constructs HUVEC were cultured for 3 days at 37°C and 5% CO_2. Where indicated, cells have also been cultured in the presence of 1mM of either UDP-GlcA or UDP-GlcNAc, freshly dissolved before use. Next, cells were fixed with 4% PFA in HBSS for 10 minutes at rT, washed in HBSS containing 1% BSA, and blocked for 30 minutes at room temperature in 5% BSA in HBSS. Ncan-dsRed was incubated overnight (at 4°C), followed by 10µg/mL Hoechst 33528, embedded in Vectashield mounting medium (Vector Laboratories Inc., Burlingame, CA). Cells were examined using a LEICA TCS SP8 X WLL (Leica, Rijswijk, The Netherlands) with a 40x objective (HC PL APO CS2 40x/1.30 oil, Leica) or LEICA TCS SP5 with a 100x objective (HCX PL APO CS 100x/1.40 oil, Leica). Sequential 16-bit confocal images (xyz dimensions, 0.142×0.142×0.3µm, 0.142×0.142×1µm or 0.116x0.116×1µm) were recorded using LAS-X Image software (Leica) and analyzed with ImageJ, as described earlier[35]. Surface hyaluronan expression (Ncan-dsRed) was quantified on 5 cells per field of view from a side-view, resliced from a line (10pixels/line wide) over the nucleus, 3 additional lines (10pixels/line) were drawn at the nuclear position as described earlier[36]. HA coverage was calculated

as average fluorescence multiplied by the distance from half-maximum signal of the nuclear staining to half-maximum signal at the luminal end.

RNA isolation and qRT-PCR analysis

Total RNA was prepared using the RNeasy RNA extraction kit with on-column DNase digestion (Qiagen, Chatsworth, CA) following the manufacturer's instructions. The DNase-treated RNA (100 ng) was then converted into cDNA using random primers and SuperScript III (Invitrogen) or M-MLV First-Strand Synthesis (Life Technologies, Carlsbad, California, USA) and stored at -80°C. qRT-PCR detection was carried out using SYBR Green Master mix (Life Technologies) and respective primers (Supplementary Table 1). Levels of expression were determined by normalization to *GAPDH* levels.

Western blot analysis

As described above, cultured HUVECs were washed with PBS and lysed in 50mM TRIS HCL buffer (pH 7.5) containing 150mM NaCl, 1% SDS, 0.5% deoxycholate and 0.5% triton X-100. Protein samples were diluted 5x in SDS sample buffer (pH 6.8; 10% SDS, 25% 2-mercaptoethanol, 50% glycerol, 0.01% bromophenol blue, 0.3125M Tris-HCl, 0.5M DTT), incubated at 95°C for 10 minutes and subjected to SDS-PAGE and western blotting. Proteins, transferred to PVDF membrane (1704156, Bio-Rad Laboratories BV, Veenendaal, The Netherlands) were detected with antibodies against HAS2 (MABC712, Merck Millipore), Pospho-Tie2 (Y1102/Y1100; AF3909, R&D Systems) and Mouse anti-Tie2 (ab24859, Abcam), and GAPDH (NB300-221SS, Novus Biologicals) after blocking the membrane with 5% fat-free milk in PBS and 0.1% Tween-20. Followed by incubation with a secondary HRP-conjugated antibody and Pierce ECL Western Blotting substrate (32106, Thermo Scientific). Band intensity was analyzed using ImageJ software.

Metabolic assays

For intracellular metabolite measurements (NMR profiling), as published in detail[37], HUVECs were cultured in EGM2 medium for 3 days in 10cm dishes until cell numbers reached about 5million per dish transduced with *Pfkfb3*^{OE}*, shPfkfb3* or respective mock controls, cultured for another 16hrs, transferred to 10cm dishes and kept further for another 3 days in culture until cell numbers reached about 5million per dish. Sample preparation was started by removing culture medium followed by quick rinsing with warm PBS (~5mL, 37˚C) to remove residual culture medium. Both the removal of medium and washing with PBS occurred in less than 5s to avoid turnover of labile intracellular metabolites. Subsequently, cells were quenched with ~10mL liquid nitrogen (LN_2) and plates were placed on dry-ice while the whole process was repeated for all samples. Prior to removal of the culture medium, an aliquot of 0.3mL was collected and immediately mixed with 0.6 mL cold methanol (-80˚C,

100% LC-grade) and stored a -80 ˚C. This treatment ensures to remove by precipitation the proteins present in the medium.

Extraction of intracellular metabolites was performed in a cold room (4˚C) using 1.5mL of methanol/chloroform/water, 8.1:0.9:1 (v/v/v) solution per plate. The extraction solution was kept cold on dry-ice throughout the whole procedure. The cells were scraped from the plates and transferred to 2mL micro-centrifuge tubes together with the extraction solvents and centrifuged at 16,000 × g for 15 min at 4˚C. The supernatants were collected, dried with nitrogen airflow and stored at -80˚C. The dried material was reconstituted with 0.25mL of 150mM K_2PO_4 buffer solution (pH = 7.4) in deuterated water (D2O; Cortecnet, France). The buffer solution included also 2mM NaN_3 to prevent bacteria contamination of the samples during storage and analysis and 0.02mM of TSP-*d4* (3-trimethylsilyl-propionate-d4 salt; Cambridge Isotope Laboratories Inc., UK) as a concentration and NMR chemical shift internal standard. Each extract-buffer mixture was vortexed for 10s and 165µL were transferred to 3mm NMR tubes (Bruker Biospin Ltd., Germany) using a 215 Gilson robotic liquid handler. 30µL from each sample leftovers were pooled and stored at -80˚C as aliquots of 180µL. These pooled samples were used for 2D NMR spectroscopy and assignment of metabolites. NMR data were recorded using a Bruker 14.1 T AVANCE II spectrometer for 1H 600 MHz, equipped with a cryoprobe (TCI) and a SampleJet system (Bruker Biospin ltd.). The latter is equipped with cooling positions to accommodate 5 × 96-tube racks so that all samples are kept at a stable temperature of 4 ˚C while in que for analysis. The same automation routine was followed for all samples and included the placement for 5 min in the probe to adopt a stable temperature at 27°C, tuning, matching, lock to the frequency of deuterium, shimming and 90˚ pulse calibration followed by the acquisition of a 1D ^{1}H NOESY and a 2D J-resolved (Jres) experiments. The 1D NOESY (doi:10.1002/cmr.a.20223) experiment (noesygppr1d experiment in Topspin 3.0 library; Bruker Biospin Ltd.) uses the first increment of the 2D NOESY pulse sequence and it was used for metabolites quantification. 512 scans were recorded for each sample with 65536 points over a 20ppm (12335 Hz) spectral width. Residual water signal was suppressed by a 50Hz continuous wave soft pulse during the relaxation delay of 4s and the mixing time of 10ms. The collected data was 2-fold zero-filled, Fourier transformed, phased and referenced to the internal standard (TSP) chemical shift at 0.0ppm. 2D Jres (http://dx.doi.org/10.1063/1.431994) were collected for the assignment of metabolites. The spectral width was set to 16.66 ppm (12288 Hz) for the direct dimension and 78Hz for the indirect one and 4 scans were acquired over 40 increments. The free induction decays (FIDs) were automatically processed with Fourier transformation and calibrated using the TSP-*d4* signal at 0.0ppm in the F2 dimension and at 0.0Hz in the F1 dimension. A set of 2D NMR spectra were recorded for the pooled samples to be used for assignment of resonances. The set of 2D experiments included ^{1}H-^{1}H correlation spectroscopy (COSY), total correlation

spectroscopy (TOCSY) and ^{1}H-^{13}C heteronuclear single quantum correlation (HSQC) using the standard parameters implemented in Topspin 3.0 (Bruker Biospin Ltd.). Identification of metabolites was performed by search of the total 1D and 2D Jres data using the Biorefcode database (Bruker Biospin Ltd.) and ChenomX NMR suite 8.1 (Chenonx Inc. Canada). The ID of the annotated resonances were further verified by the collected 2D NMR data. In cases of ambiguous annotation, spiking experiments of reference samples were performed to confirm the metabolites ID. Quantification of the identified metabolites was performed with the ChenomX NMR suite 8.1 software. Concentrations were extracted using the known TSP-*d4* concentration (0.017mM) and corrected to sample protein concentration. The exact concentration of the internal standard used for quantification was calculated by the ERETIC2 method implemented in Topspin 3.0 (Bruker Biospin Ltd.).

To measure endothelial glycolytic flux, HUVECs were seeded overnight at 60,000 cells per well on fibronectin (Sigma) coated Seahorse XF96 polystyrene tissue culture plates (Seahorse Bioscience). The plate was incubated in unbuffered DMEM assay medium (Sigma) for 1 hour in a non-CO_2 incubator at 37°C before measuring in an XFe 96 extracellular flux analyzer (Seahorse Bioscience). Both OCR (oxygen consumption rate) and extracellular acidification rate (ECAR) were measured over 4min periods with a mixing of 2min in each cycle, with five cycles in total. Inhibitors and activators were used at the following concentrations: Glucose (10mM), Oligomycin (3µM), 2-DG (100mM), FCCP (1µM), Antimycin A (1.5µM) and Rotenone (3µM). Cellular protein content was determined with a BCA-protein kit from Pierce (Thermo-Fischer Scientific) and the data is represented as ECAR and OCR normalized to protein. Each measurement was averaged from triplicate wells.

Statistical analysis

Results are presented as mean ± s.d. or mean ± s.e.m., n defines the number of biological replicates. Differences between groups were assessed by non-paired 2-tailed Student's t test, paired 2-tailed Student's t test or, when not normally distributed, by two-tailed F-test. P values < 0.05 were considered statistically significant.

Results

Endothelial glycocalyx HA presence is reduced in melanoma liver metastatic capillaries

In vivo, glycolysis is increased in tumor ECs, whereby glycolytic intermediates are diverted into the pentose phosphate pathway (PPP) and serine biosynthesis pathway (SBP) to promote nucleotide synthesis [9]. Since this could directly influence the synthesis of HA substrates, we evaluated endothelial surface HA presence in melanoma liver metastatic capillaries and compared these levels to quiescent

liver sinusoid endothelial surface coverage. In metastatic capillaries, luminal HA was ~50% reduced from the endothelial surface (Fig. 1a and 1b). This substantial loss of the glycocalyx structure was further corroborated through reduced lectin binding of LEA-FITC on the endothelial surface (Fig. 1a and 1c). Detailed observations of a tumor vessel stained for HA clearly revealed such loss of HA expression along the line from basement up to the intraluminal tip of an angiogenic endothelial cell (Fig. 1d and 1e). To further confirm it, we isolated tumor endothelial cells (TECs) and measured the surface HA presence *in vitro*. In comparison to normal endothelial cells, tumor endothelial cells express less surface HA (Fig. 1f and 1g).

Endothelial HA synthesis is dependent on glycolytic PFKFB3 activity

Endothelial expression of Krüppel-Like Factor 2 (KLF2) and its inhibitory effect on the glycolytic activator phosphofructokinase-2/fructose-2,6-bisphosphatase-3 (PFKFB3), have been shown to be important regulators of endothelial quiescence and vessel stabilization [38]. Further, HA synthesis requires the substrates UDP-GlcA and UDP-GlcNAc, produced from the glycolytic intermediate glucose-6-phosphate. Hence, we hypothesized that a high glycolysis flux in ECs can shift glucose-6-phosphate away from the metabolic pathways that produce UDP-GlcA and UDP-GlcNAc. Because of these reasons, we tested whether changes in endothelial metabolism affected HA biosynthesis.

First, static cultured ECs that overexpress the glycolytic activator PFKFB3 ($PFKFB3^{OE}$) show elevated *PFKFB3* mRNA expression, without however affecting HAS2 protein levels (Supplementary Fig. 1a-b). Extracellular acidification rate (ECAR), as an indicator of lactate production, showed increased glycolysis and maximal glycolytic capacity upon overexpression of PFKFB3 in ECs (Fig. 2a,b) defined as ECAR induced by the mitochondrial respiration blocker oligomycin to force the cells to rely more on glycolysis. $PFKFB3^{OE}$ was at the same time also accompanied by reduced mitochondrial respiration (Fig. 2c,d). $PFKFB3^{OE}$ increased the levels of the glycolytic end-product lactate (Fig. 2h) and reduced levels of extracellular glucose, indicating enhanced glucose consumption (Fig. 2e). Activation of glycolysis slightly reduced intracellular glucose (Glc) (Fig. 2f), without changing the levels of the intermediate UDP-Glc (Fig. 2g), while both substrates for HA synthesis, UDP-GlcNAc and UDP-GlcA, were reduced significantly (Fig. 2i). This resulted in reduced luminal HA at the endothelial surface, which could be rescued by supplementing the HA substrates UDP-GlcNAc and UDP-GlcA (Fig. 2j and 2k) to increase their cytosolic pool (Supplementary Fig. 2a-d). Together, these data show that PFKFB3 activity modulates intracellular substrate availability for HA synthesis and hence endothelial glycocalyx coverage.

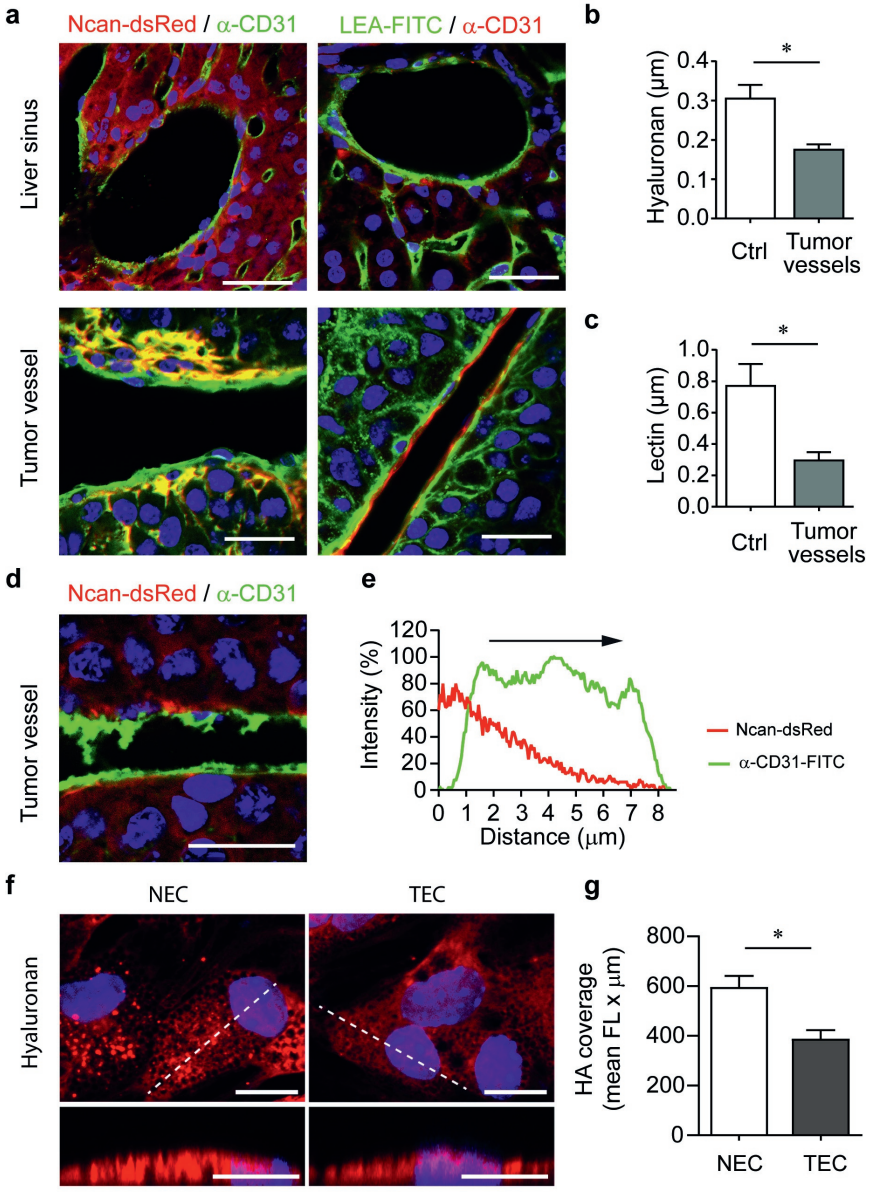

Figure 1. Endothelial glycocalyx HA presence is reduced in melanoma liver metastatic capillaries. (a) Representative confocal images of liver tissue adjacent to metastatic tissue of B16-F10 melanoma cancer cells stained for the luminal glycocalyx with the hyaluronan binding probe Ncan-dsRed (red, left) or stained for the luminal glycocalyx with the lectin Lycopersicon esculentum (LEA-FITC, green, right) and antibodies against CD31 for endothelial localization. Scale bars 30μm. **(b)** Quantification of

endothelial luminal HA coverage within liver sinus or tumor vessels in WT mice (n = 3-6/group). **(c)** Quantification of endothelial luminal lectin coverage within liver sinus or tumor vessels in WT mice (n = 3-6/group). **(d)** Detailed confocal image of a tumor vessel stained for hyaluronan (Ncan-dsRed) and endothelial cells (CD31), annotated with an arrow of which **(e)** the luminal distribution of hyaluronan is shown throughout the intraluminal tip of the angiogenic endothelial cell. **(f)** Representative confocal images of HA staining in normal endothelial cells (NEC) and tumor endothelial cells (TEC). **(g)** quantification of surface HA. Values are given as mean ± s.d. and differences between non-tumor liver sinus and tumor vessels in WT mice were assessed by paired 2-tailed Student's *t*-test; *P < 0.05.

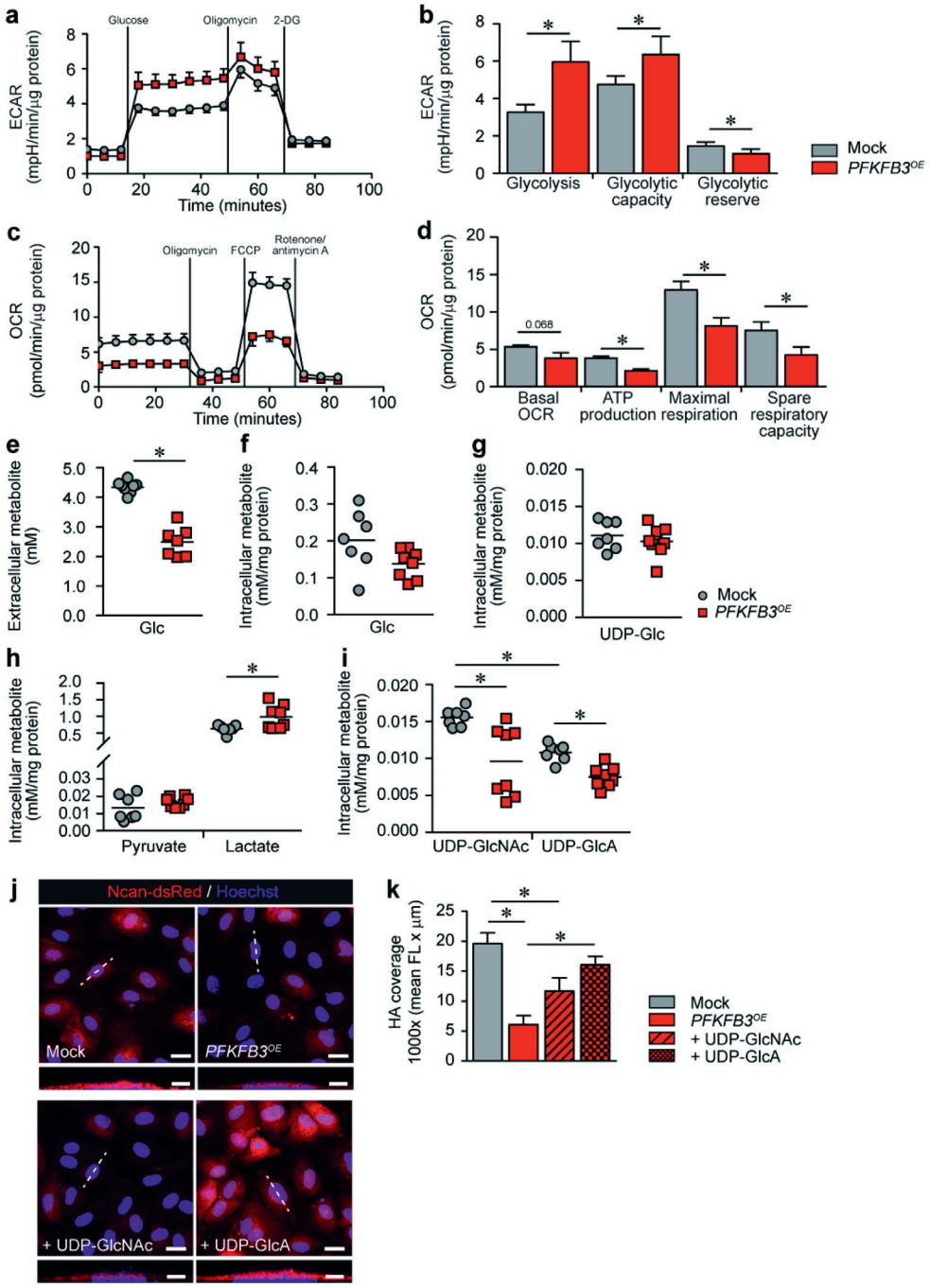

Figure 2. Increased endothelial PFKFB3 activity results in reduced hyaluronan biosynthesis. To test whether changes in endothelial metabolism affects HA biosynthesis, HUVECs are cultured overexpressing the glycolytic activator PFKFB3 (PFKFB3^{OE}). **(a)** Using a Seahorse XF flux analyzer the

extracellular acidification rate (ECAR) showed a raise in anaerobic glycolysis in PFKFB3^{OE} cells, which resulted in an **(b)** absolute increase in basal glycolysis, glycolytic capacity and glycolytic reserve (n = 4). **(c)** Oxygen consumption rate (OCR) in these cells was reduced in comparison to control, especially **(d)** ATP production, maximal mitochondrial respiration and its spare respiratory capacity. Quantitative glycolytic metabolites measurements using NMR showed that **(e)** extracellular glucose (Glc) was significantly reduced in PFKFB3^{OE} cells. While intracellular **(f)** glucose-, **(g)** UDP-glucose- (UDP-Glc) and **(h)** pyruvate- metabolite concentrations were not affected, a clear increase was observed in intracellular lactate. These glycolytic changes revealed significantly reduced intracellular levels of both **(i)** HA substrates, UDP-GlcNAc and UDP-GlcA (n = 8/group). Confirmation of these results was obtained measuring HA coverage on the luminal surface of PFKFB3^{OE} cells. **(j)** Representative images show control ECs (Mock), PFKFB3^{OE} cells or PFKFB3^{OE} cells cultured for the final 24hrs in the presence of 1mM UDP-GlcNAc or UDP-GlcA (bottom panels). Scale bars, 20µm. **(k)** PFKFB3 overexpression significantly reduced luminal endothelial hyaluronan coverage which could be restored partially by addition of UDP-GlcNAc and even further with UDP-GlcA (n = 4/group). Values are given as mean ± s.e.m (b,d,k) or mean ± s.d. (a,c) and differences between Mock and PFKFB3^{OE} cells were assessed by paired- (b,d) or non-paired 2-tailed Student's t test; *P < 0.05.

Reduction of endothelial PFKFB3 expression increases endothelial HA coverage

We then explored whether inhibition of endothelial glycolysis might be useful to promote glycocalyx formation. We therefore analyzed HA expression in tumor ECs in *Pfkfb3*$^{+/\Delta EC}$ mice, a mouse model in which one allele of the PFKFB3 gene is inactivated in ECs in a tamoxifen-inducible manner [9]. In comparison to WT mice, luminal HA expression was nearly doubled in tumor ECs from *Pfkfb3*$^{+/\Delta EC}$ mice (Fig. 3a, top row and 3b) and was accompanied by increased lectin staining (Fig. 3a, top row and 3c). *In vitro*, silencing PFKFB3 (shPFKFB3) significantly reduced *PFKFB3* mRNA levels and increased endothelial HA coverage (Fig. 3d and 3e), however, without changing total HAS2 protein levels (Supplementary Fig. 1c-d). This further mechanistically corroborates the dependency of PFKFB3 acivity for tumor endothelium HA/glycocalyx synthesis.

PFKFB3 activation is associated with vessel destabilization

Tumor ECs in *Pfkfb3*$^{+/\Delta EC}$ mice exhibit signs of tumor vessel normalization, characterized by EC stabilization[9]. To test the hypothesis that this could be related to restoration of endothelial HA/glycocalyx production and related restoration of Ang1/Tie2 signaling we compared WT to *Pfkfb3*$^{+/\Delta EC}$ mice. Gross Ang1 staining on tumor endothelium in the two mice models did not reveal

significant differences, most likely because this assay is not sufficiently sensitive to detect such changes (Fig. 4a, left panels and 4b). However, there was clearly enhanced Tie2 receptor phosphorylation in *Pfkfb3*$^{+/\Delta EC}$ mice (Fig. 4a, right panels and 4c), which has been implicated in vessel stabilisation [39]. To confirm the mechanistic role of PFKFB3 in this observation, we phenocopied tumor endothelium by overexpressing PFKFB3 (PFKFB3^{OE}). PFKFB3^{OE} in these cells, cultured in the presence of Ang1, not only decreased luminal HA expression, but also reduced the luminal presence of Ang1 (Fig. 4d and 4e). As a result, activation of its receptor Tie-2 was reduced (Fig. 4f and 4g).

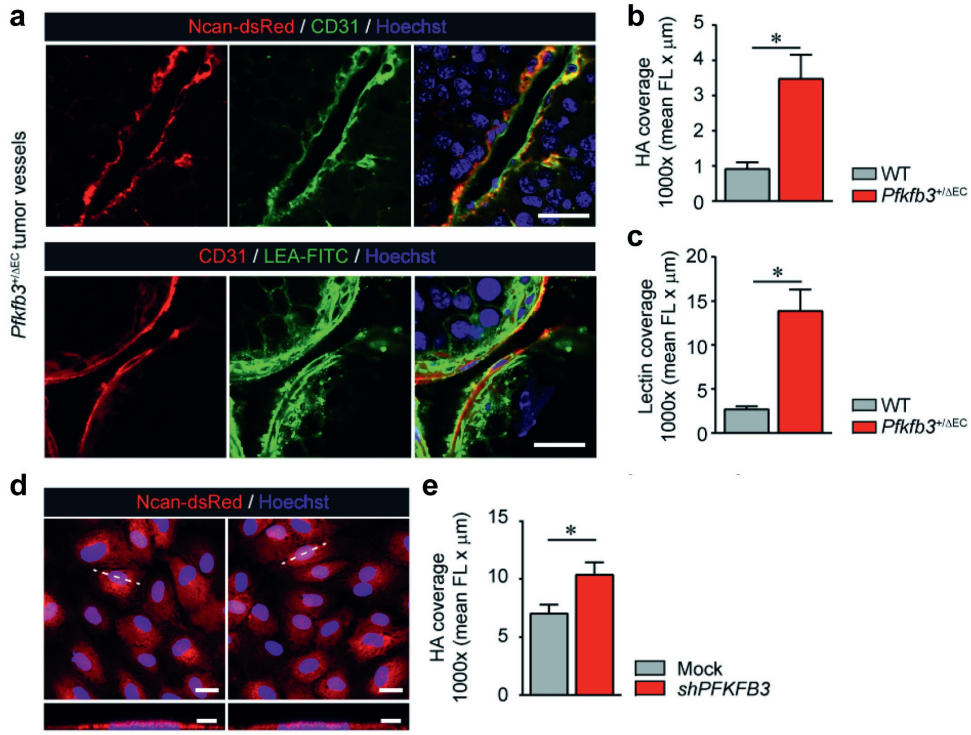

Figure 3. Reduction of PFKFB3 expression increases HA presence in vivo and in vitro. (a) Representative confocal images of B16-F10 melanoma metastatic capillaries in *Pfkfb3*$^{+/\Delta EC}$ mice in which endothelial glycolysis rate is genetically reduced. Tissues are stained for the luminal glycocalyx with Ncan-dsRed (upper panels) or LEA-FITC (lower panels) and antibodies against CD31 for endothelial localization. Scale bars 30µm. Quantification of endothelial **(b)** luminal HA or **(c)** lectin expression in tumor vessels of WT and Pfkfb3+/ΔEC mice (n = 3-6/group). **(d)** Representative images depicting control HUVECs (Mock, left) or, *shPFKFB3* (right) cells. Scale bars, 20µm. **(e)** Silencing *PFKFB3* significantly increased luminal endothelial hyaluronan coverage (*n = 4/group*). Values are given as mean ± SD of 3-6 independent experiments. Non-paired 2-tailed Student's t test was performed; *P < 0.05.

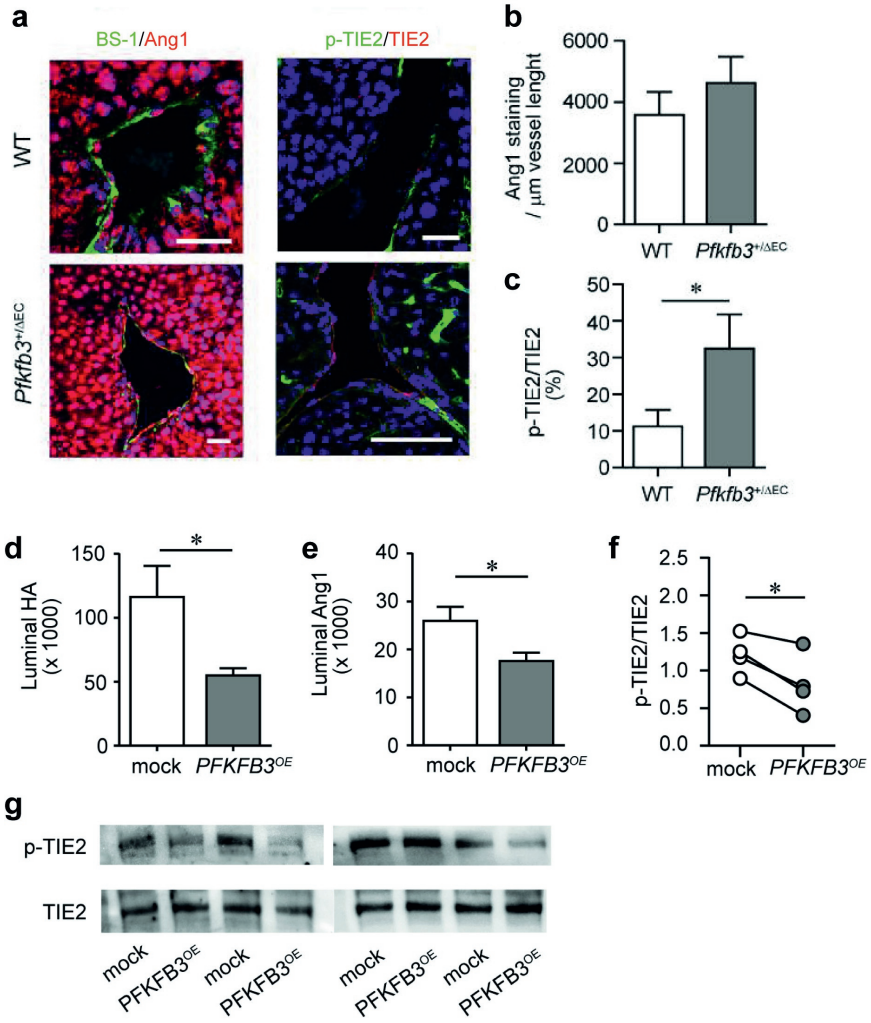

Figure 4. Endothelial glycolytic activation reduces endothelial HA coverage and is associated with reduced vascular Tie2 activation. (a) Representative confocal images of B16-F10 melanoma metastatic capillaries in WT or in Pfkfb3+/ΔEC mice stained for the endothelial angiopoietin 1 (Ang1, red) and the Griffonia simplicifolia (isolectin BS-1, green) lectin for endothelial localization (left panels), or for endothelial bound p-Tie2(Y1102, red) and Tie2 (green) presence. **(b)** Quantification of endothelial luminal Ang1 expression in tumor vessels of WT and Pfkfb3+/ΔEC mice (n = 4-5/group) or **(c)** ratio of endothelial p-Tie2 over Tie2 staining. Scale bars 30µm. Primary human glomerular-derived microvascular endothelial cells (hgMVEC), transduced with an empty- (mock) or a PFKFB3OE lenti-viral construct, exposed to a laminar shear stress of 5 dyne/cm2 for 3 days in the presence of 100ng/mL recombinant human Ang1 reveals a reduced luminal **(d)** hyaluronan and **(e)** angiopoietin1 (Ang1)

presence that was accompanied with reduced Tie2 activation as shown **(f)** by quantification of p-Tie2(Y1102) over Tie2 expression from western blot **(g)**. Values are given as mean ± SD. Non-paired 2-tailed Student's t test was performed; *P < 0.05.

Discussion

The key findings of our study are: 1] Tumor endothelium is characterized by loss of HA /glycocalyx 2] high PFKFB3 mediated glycolytic activity impairs the formation of the endothelial HA/glycocalyx layer by reducing the availability of UDP-GlcA and UDP-GlcNAc, substrates for HA synthesis; 2] Reducing PFKFB3 activity in tumor endothelium restores Ang1/Tie2 receptor signalling which is required for vessel normalisation in tumor tissue [9, 39].

HA is a nonsulfated glycosaminoglycan composed of repeating polymeric disaccharides D-glucuronic acid and N-acetyl-D-glucosamine linked by a glucuronic bond [40]. HA is synthesized by membrane bound synthases (HAS1, 2 and 3) as a macromolecule with a molecular weight between 10^5 and 10^7 Dalton, thus requiring large amounts of available substrate in the cytosol. The cytosolic domains of membrane-bound HAS2 adds UDP-GlcA and UDP-GlcNAc alternately onto the reducing end of the HA chain at the expense of removing the anchoring UDP. The cellular content of UDP-GlcNAc is the highest among the different nucleotide sugars, as also shown in the current study. However, the HAS K_m for UDP-GlcNAc is also relatively high, necessitating high abundance of this substrate for efficient hyaluronan synthesis [41]. These enzyme kinetics link HA synthesis directly to metabolic glucose regulation [42].

ECs have a predominance of glycolysis for sugar metabolism, which probably allows the adaptation of the vasculature to hypoxia [10]. Indeed, EC proliferation and neo-angiogenesis are characterized by further endothelial activation of glycolysis through enhanced expression of the activator PFKFB3 [9]. This is of relevance e.g. for tumor angiogenesis, where PFKB3 activity is increased and results in glycolytic activation and vessel destabilisation [9]. Here, we extend these observations, by showing that PFKFB3 activation lowers cytosolic UDP-GlcNAc and UDP-GlcA pools and thereby impairs HA synthesis, thus interfering with Ang-1-Tie2 signalling. Our findings that endothelial haplodeficiency of PFKFB3 increases HA synthesis and glycocalyx formation in tumor ECs, in association with enhanced Ang1/Tie2 signaling and tumor vessel normalization, provides genetic proof of evidence that inhibition of endothelial glycolysis by pharmacological PFKFB3 blockade may be of therapeutic benefit to promote EC stabilization and vessel homeostasis / normalization.

These observations provide a rationale to explore endothelial glucose metabolism and consequently HA synthesis as a target for microvascular stabilisation. This is probably not only of relevance for tumor

angiogenesis, but may reflect a more general principle that can also be observed in other situations with endothelial cell activation such as diabetes or absence of normal shear (as occurs in atherosclerosis). Together, the present study expands the current concepts of endothelial metabolic homeostasis and vascular stability placing the high glycolytic flux of quiescent endothelial cells in key of regulating glycocalyx biosynthesis, in particular the presence of hyaluronan. Consequently, we conclude that HA plays a pivotal role in stabilisation of the Ang1 / Tie2 interaction on its surface and induction of downstream signalling. Loss of endothelial glycocalyx hyaluronan therefore, which leads to cell-cell contact destabilization can result in either endothelial rarefaction or angiogenesis (in a tumor environment).

Sources of Funding

Financial Support by the Dutch Kidney Foundation (grants C08.2265) and the China Scholarship Council grant to Gangqi Wang (CSC no. 201406170050) are gratefully acknowledged.

Disclosure

None.

References

[1] Dane MJ, van den Berg BM, Lee DH, Boels MG, Tiemeier GL, Avramut MC, van Zonneveld AJ, Van der Vlag J, Vink H, Rabelink TJ: A microscopic view on the renal endothelial glycocalyx. Am J Physiol Renal Physiol 2015:ajprenal 00532 2014.
[2] Rabelink AJ, van den Berg BM, Garsen M, Wang G, Elkin M, van der Vlag J: Heparanase: roles in cell survival, extracellular matrix remodelling and the development of kidney disease. Nature reviews Nephrology 2017.
[3] Rai S, Nejadhamzeeigilani Z, Gutowski NJ, Whatmore JL: Loss of the endothelial glycocalyx is associated with increased E-selectin mediated adhesion of lung tumour cells to the brain microvascular endothelium. Journal of experimental & clinical cancer research : CR 2015, 34:105.
[4] Rabelink TJ, de Zeeuw D: The glycocalyx--linking albuminuria with renal and cardiovascular disease. Nature reviews Nephrology 2015, 11:667-76.
[5] Tarbell JM, Cancel LM: The glycocalyx and its significance in human medicine. Journal of internal medicine 2016.
[6] Han S, Lee SJ, Kim KE, Lee HS, Oh N, Park I, Ko E, Oh SJ, Lee YS, Kim D, Lee S, Lee DH, Lee KH, Chae SY, Lee JH, Kim SJ, Kim HC, Kim S, Kim SH, Kim C, Nakaoka Y, He Y, Augustin HG, Hu J, Song PH, Kim YI, Kim P, Kim I, Koh GY: Amelioration of sepsis by TIE2 activation-induced vascular protection. Science translational medicine 2016, 8:335ra55.
[7] Becker BF, Jacob M, Leipert S, Salmon AH, Chappell D: Degradation of the endothelial glycocalyx in clinical settings: searching for the sheddases. British journal of clinical pharmacology 2015, 80:389-402.
[8] Rabelink TJ, van den Berg BM, Garsen M, Wang G, Elkin M, van der Vlag J: Heparanase: roles in cell survival, extracellular matrix remodelling and the development of kidney disease. Nat Rev Nephrol 2017, 13:201-12.
[9] Cantelmo AR, Conradi LC, Brajic A, Goveia J, Kalucka J, Pircher A, Chaturvedi P, Hol J, Thienpont B, Teuwen LA, Schoors S, Boeckx B, Vriens J, Kuchnio A, Veys K, Cruys B, Finotto L, Treps L, Stav-Noraas TE, Bifari F, Stapor P, Decimo I, Kampen K, De Bock K, Haraldsen G, Schoonjans L, Rabelink T, Eelen G, Ghesquiere B, Rehman J, Lambrechts D, Malik AB, Dewerchin M, Carmeliet P: Inhibition of the Glycolytic Activator PFKFB3 in Endothelium Induces Tumor Vessel Normalization, Impairs Metastasis, and Improves Chemotherapy. Cancer Cell 2016, 30:968-85.
[10] Eelen G, de Zeeuw P, Simons M, Carmeliet P: Endothelial Cell Metabolism in Normal and Diseased Vasculature. Circulation research 2015, 116:1231-44.
[11] Verdegem D, Moens S, Stapor P, Carmeliet P: Endothelial cell metabolism: parallels and divergences with cancer cell metabolism. Cancer Metab 2014, 2:19.
[12] Carmeliet P, Jain RK: Molecular mechanisms and clinical applications of angiogenesis. Nature 2011, 473:298-307.
[13] Cerutti C, Ridley AJ: Endothelial cell-cell adhesion and signaling. Experimental cell research 2017.
[14] Jain RK: Antiangiogenesis strategies revisited: from starving tumors to alleviating hypoxia. Cancer cell 2014, 26:605-22.
[15] Carmeliet P, Jain RK: Principles and mechanisms of vessel normalization for cancer and other angiogenic diseases. Nature reviews Drug discovery 2011, 10:417-27.
[16] Sarrazin S, Lamanna WC, Esko JD: Heparan sulfate proteoglycans. Cold Spring Harbor perspectives in biology 2011, 3.
[17] Bishop JR, Schuksz M, Esko JD: Heparan sulphate proteoglycans fine-tune mammalian physiology. Nature 2007, 446:1030-7.
[18] Vigetti D, Karousou E, Viola M, Deleonibus S, De Luca G, Passi A: Hyaluronan: biosynthesis and signaling. Biochimica et biophysica acta 2014, 1840:2452-9.
[19] Matsumoto K, Li Y, Jakuba C, Sugiyama Y, Sayo T, Okuno M, Dealy CN, Toole BP, Takeda J, Yamaguchi Y, Kosher RA: Conditional inactivation of Has2 reveals a crucial role for hyaluronan in

skeletal growth, patterning, chondrocyte maturation and joint formation in the developing limb. Development 2009, 136:2825-35.
[20] Tammi RH, Passi AG, Rilla K, Karousou E, Vigetti D, Makkonen K, Tammi MI: Transcriptional and post-translational regulation of hyaluronan synthesis. The FEBS journal 2011, 278:1419-28.
[21] Vigetti D, Viola M, Karousou E, De Luca G, Passi A: Metabolic control of hyaluronan synthases. Matrix biology : journal of the International Society for Matrix Biology 2014, 35:8-13.
[22] Vigetti D, Ori M, Viola M, Genasetti A, Karousou E, Rizzi M, Pallotti F, Nardi I, Hascall VC, De Luca G, Passi A: Molecular cloning and characterization of UDP-glucose dehydrogenase from the amphibian Xenopus laevis and its involvement in hyaluronan synthesis. The Journal of biological chemistry 2006, 281:8254-63.
[23] Baggenstoss BA, Harris EN, Washburn JL, Medina AP, Nguyen L, Weigel PH: Hyaluronan synthase control of synthesis rate and hyaluronan product size are independent functions differentially affected by mutations in a conserved tandem B-X7-B motif. Glycobiology 2016, 27:154-64.
[24] Viola M, Karousou E, D'Angelo ML, Caon I, De Luca G, Passi A, Vigetti D: Regulated Hyaluronan Synthesis by Vascular Cells. International journal of cell biology 2015, 2015:208303.
[25] Slawson C, Copeland RJ, Hart GW: O-GlcNAc signaling: a metabolic link between diabetes and cancer? Trends in biochemical sciences 2010, 35:547-55.
[26] De Bock K, Georgiadou M, Carmeliet P: Role of endothelial cell metabolism in vessel sprouting. Cell metabolism 2013, 18:634-47.
[27] Augustin HG, Koh GY, Thurston G, Alitalo K: Control of vascular morphogenesis and homeostasis through the angiopoietin-Tie system. Nature reviews Molecular cell biology 2009, 10:165-77.
[28] Thurston G, Rudge JS, Ioffe E, Zhou H, Ross L, Croll SD, Glazer N, Holash J, McDonald DM, Yancopoulos GD: Angiopoietin-1 protects the adult vasculature against plasma leakage. Nature medicine 2000, 6:460-3.
[29] Campochiaro PA, Peters KG: Targeting Tie2 for Treatment of Diabetic Retinopathy and Diabetic Macular Edema. Current diabetes reports 2016, 16:126.
[30] Wong AL, Haroon ZA, Werner S, Dewhirst MW, Greenberg CS, Peters KG: Tie2 expression and phosphorylation in angiogenic and quiescent adult tissues. Circulation research 1997, 81:567-74.
[31] van den Berg BM, Wang G, Boels MGS, Avramut MC, Jansen E, Sol W, Lebrin F, Jan van Zonneveld A, de Koning EJP, Vink H, Grone HJ, Carmeliet P, van der Vlag J, Rabelink TJ: Glomerular Function and Structural Integrity Depend on Hyaluronan Synthesis by Glomerular Endothelium. J Am Soc Nephrol 2019, 30:1886-97.
[32] De Bock K, Georgiadou M, Schoors S, Kuchnio A, Wong BW, Cantelmo AR, Quaegebeur A, Ghesquiere B, Cauwenberghs S, Eelen G, Phng LK, Betz I, Tembuyser B, Brepoels K, Welti J, Geudens I, Segura I, Cruys B, Bifari F, Decimo I, Blanco R, Wyns S, Vangindertael J, Rocha S, Collins RT, Munck S, Daelemans D, Imamura H, Devlieger R, Rider M, Van Veldhoven PP, Schuit F, Bartrons R, Hofkens J, Fraisl P, Telang S, Deberardinis RJ, Schoonjans L, Vinckier S, Chesney J, Gerhardt H, Dewerchin M, Carmeliet P: Role of PFKFB3-driven glycolysis in vessel sprouting. Cell 2013, 154:651-63.
[33] Zhang H, Baader SL, Sixt M, Kappler J, Rauch U: Neurocan-GFP fusion protein: a new approach to detect hyaluronan on tissue sections and living cells. J Histochem Cytochem 2004, 52:915-22.
[34] Jaffe EA, Nachman RL, Becker CG, Minick CR: Culture of human endothelial cells derived from umbilical veins. Identification by morphologic and immunologic criteria. The Journal of clinical investigation 1973, 52:2745-56.
[35] Dane MJ, van den Berg BM, Avramut MC, Faas FG, van der Vlag J, Rops AL, Ravelli RB, Koster BJ, van Zonneveld AJ, Vink H, Rabelink TJ: Glomerular endothelial surface layer acts as a barrier against albumin filtration. The American journal of pathology 2013, 182:1532-40.
[36] Boels MG, Avramut MC, Koudijs A, Dane MJ, Lee DH, van der Vlag J, Koster AJ, van Zonneveld AJ, van Faassen E, Grone HJ, van den Berg BM, Rabelink TJ: Atrasentan Reduces Albuminuria by Restoring the Glomerular Endothelial Glycocalyx Barrier in Diabetic Nephropathy. Diabetes 2016, 65:2429-39.

[37] Kostidis S, Addie RD, Morreau H, Mayboroda OA, Giera M: Quantitative NMR analysis of intra- and extracellular metabolism of mammalian cells: A tutorial. Analytica chimica acta 2017, 980:1-24.
[38] Doddaballapur A, Michalik KM, Manavski Y, Lucas T, Houtkooper RH, You X, Chen W, Zeiher AM, Potente M, Dimmeler S, Boon RA: Laminar shear stress inhibits endothelial cell metabolism via KLF2-mediated repression of PFKFB3. Arteriosclerosis, thrombosis, and vascular biology 2015, 35:137-45.
[39] Park JS, Kim IK, Han S, Park I, Kim C, Bae J, Oh SJ, Lee S, Kim JH, Woo DC, He YL, Augustin HG, Kim I, Lee D, Koh GY: Normalization of Tumor Vessels by Tie2 Activation and Ang2 Inhibition Enhances Drug Delivery and Produces a Favorable Tumor Microenvironment. Cancer Cell 2016, 30:953-67.
[40] Laurent TC, Fraser JR: Hyaluronan. FASEB journal : official publication of the Federation of American Societies for Experimental Biology 1992, 6:2397-404.
[41] Itano N, Sawai T, Yoshida M, Lenas P, Yamada Y, Imagawa M, Shinomura T, Hamaguchi M, Yoshida Y, Ohnuki Y, Miyauchi S, Spicer AP, McDonald JA, Kimata K: Three isoforms of mammalian hyaluronan synthases have distinct enzymatic properties. The Journal of biological chemistry 1999, 274:25085-92.
[42] Wang A, Hascall VC: Hyperglycemia, intracellular hyaluronan synthesis, cyclin D3 and autophagy. Autophagy 2009, 5:864-5.

Supplemental figures

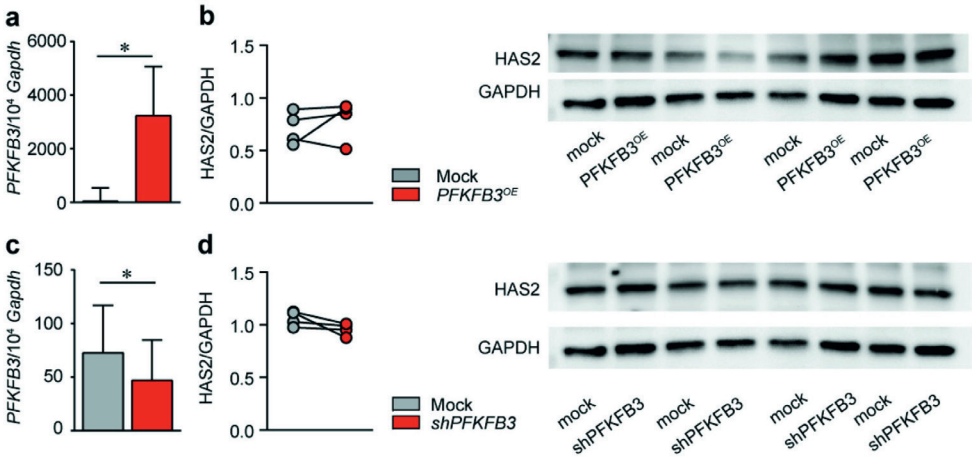

Supplemental figure 1. Changes in endothelial PFKFB3 occur without changes in endothelial HAS2 expression. (a) qPCR analysis of PFKFB3$_{OE}$ transduction revealed highly elevated *PFKFB3* mRNA expression without affecting **(b)** HAS2 protein levels, as quantified from Western-Blot (n = 4). **(c)** qPCR analysis of shPFKFB3 transduction revealed reduced *PFKFB3* mRNA expression without affecting **(d)** HAS2 protein levels, as quantified from Western-Blot (n = 4). Values are given as mean ± SD of 3-4 independent experiments. Non-paired 2-tailed Student's t test was performed; *P < 0.05.

Supplemental Tables

Table I Primers used for RT-PCR

	Forward (5'-3')	*Reverse (5'-3')*	*Product (bp)*
GAPDH	TTCCAGGAGCGAGATCCCT	CACCCATGACGAACATGGG	*195*
HAS2	AAGAACAACTTCCACGAAAAGGG	GGCTGGGTCAAGCATAGTGT	*216*
PFKFB3	CAGTTGTGGCCTCCAATATC	GGCTTCATAGCAACTGATCC	*113*